

# Inflight Characterization of the Cassini Spacecraft Propellant Slosh and Structural Frequencies

Allan Y. Lee\* and Joan Stupik†  
*Jet Propulsion Laboratory, California Institute of Technology*

While there has been extensive theoretical and analytical research regarding the characterization of spacecraft propellant slosh and structural frequencies, there have been limited studies to compare the analytical predictions with measured flight data. This paper uses flight telemetry from the Cassini spacecraft to get estimates of high-g propellant slosh frequencies and the magnetometer boom frequency characteristics, and compares these values with those predicted by theoretical works. Most Cassini attitude control data are available at a telemetry frequency of 0.5 Hz. Moreover, liquid sloshing is attenuated by propellant management device and attitude controllers. Identification of slosh and structural frequency are made on a best-effort basis. This paper reviews the analytical approaches that were used to predict the Cassini propellant slosh frequencies. The predicted frequencies are then compared with those estimated using telemetry from selected Cassini burns where propellant sloshing was observed (such as the Saturn Orbit Insertion burn). Determination of the magnetometer boom structural frequency is also discussed.

## Acronyms

<i>DSM</i>	=	deep space maneuver
<i>MMH</i>	=	monomethylhydrazine
<i>MOI</i>	=	moment of inertia
<i>NTO</i>	=	nitrogen tetroxide
<i>OTM</i>	=	orbit trim maneuver
<i>PMD</i>	=	propellant management device
<i>PRM</i>	=	periapsis raise maneuver
<i>RCS</i>	=	reaction control system
<i>RPWS</i>	=	radio and plasma wave science
<i>RWA</i>	=	reaction wheel assembly
<i>SOI</i>	=	Saturn orbit insertion
<i>TCM</i>	=	trajectory correction maneuver

## Nomenclature

$a$	=	acceleration, $\text{m/s}^2$
$d$	=	diameter of a propellant tank, m
$e_z$	=	Z-axis attitude control error, mrad
$f$	=	frequency of a time signal, Hz
$I_{zz}$	=	Z-axis moment of inertia of spacecraft, $\text{kg}\cdot\text{m}^2$
$R$	=	radius of a propellant tank, m

---

\*Section Staff, Guidance and Control Section, Division of Autonomous Systems. Mail Stop 230-104, 4800 Oak Grove Drive, Pasadena, CA 91109-8099, USA. Allan.Y.Lee@jpl.nasa.gov.

†Cassini Spacecraft Operations Office, Jet Propulsion Laboratory, Mail Stop 230-104, 4800 Oak Grove Drive, Pasadena, California 91109-8099, USA. Joan.Stupik@jpl.nasa.gov.

$T_{\text{env}}$	=	environmental torque, N-m
$\xi$	=	damping ratio, -
$\rho$	=	linear density of a spacecraft boom, kg/m
$\sigma$	=	surface tension coefficient, N/m
$\omega$	=	spacecraft angular rate, rad/s
$\Omega$	=	frequency of a flexible body, rad/s

## I. Introduction

A sophisticated interplanetary spacecraft, Cassini is one of the largest spacecraft humans have ever built and launched (see Fig. 1).<sup>1,2</sup> Since achieving orbit at Saturn in 2004, Cassini has collected science data throughout its four-year prime mission (2004–08), and has since been approved for a first and second extended missions through September 2017. The orbiter is about 6.8 m in height with a “diameter” of 4 meters. The total mass of the spacecraft at launch was approximately 5,574 kg, which included about 3,000 kg of bi-propellant. Cassini is a flexible spacecraft with four structural appendages and three propellant tanks. The four appendages are the 10-m magnetometer boom and three similar radio and plasma wave science (RPWS) antennas. Fig. 1 depicts the Cassini spacecraft with the deployed magnetometer and RPWS antennas.<sup>2</sup> The fundamental frequency of the magnetometer boom is 0.67 Hz and that of the RPWS antennas is 0.13 Hz.<sup>1</sup> A modal test was performed on the Cassini spacecraft at the Jet Propulsion Laboratory in August 1995 to provide experimental data for the verification of the finite element model (FEM) of the spacecraft in its launch configuration.<sup>3</sup> Frequencies of the primary bending modes of the spacecraft range 7.51–7.75 Hz, while the primary torsional mode frequency is 15.52 Hz. All other structural mode frequencies are higher than 20 Hz.<sup>3</sup> Cassini is a “structurally rigid” spacecraft.

The Cassini propulsion module houses two cylindrical tanks with hemispherical end domes (see Fig. 2, from Ref. 4). These tanks each contain an eight-panel propellant management device (PMD) of the surface tension type. Key functions performed by the Cassini PMD are: [1] to facilitate high-efficiency gas-free expulsion of liquid, [2] to control the propellant c.m. to within several centimeters of the tanks’ centerlines, especially after a spacecraft slew to align engine thrust with the desired burn attitude, and [3] to increase the liquid slosh frequency and slosh damping, and to decrease the slosh participatory mass fraction. When the Cassini main engine is fired to achieve a  $\Delta V$ , the resultant spacecraft translational acceleration achieved by the 445-N main engine is large enough so that the surface tension forces do not significantly affect the propellant motion during main engine burns, and the situation is referred to as a “high-g” mode. When the spacecraft attitude is controlled by a set of three reaction wheels or eight 1-N (blowdown) thrusters, the bipropellant is in a so-called “low-g” sloshing mode. Predicted performance of the low-g and high-g propellant slosh modes, described in details in Ref. 4, will be briefly reviewed in Section II. The monopropellant for Cassini is hydrazine, with 132.1 kg at launch carried by a single spherical tank (see Fig.1). This tank contains an elastomeric diaphragm for expulsion of hydrazine in zero-g condition.

The Cassini Attitude and Articulation Control System (AACS) estimates and controls the attitude of the three-axis stabilized Cassini spacecraft. Attitude determination sensors used by Cassini AACS include two Stellar Reference Units (SRU, or star trackers), two Sun Sensor Assemblies, and two Inertial Reference Units (IRU, or gyroscopes).<sup>1</sup> The AACS responds to ground-commanded pointing goals for the science instruments. To point to the commanded targets within the required accuracy, AACS uses either thrusters or reaction wheels to control the spacecraft’s attitude. The design of the RWA control system for the Cassini spacecraft is described in Ref. 5 and the references cited therein. The bandwidths of the RWA (reaction wheel assembly) and RCS (reaction control system) controllers are 0.0299 and 0.15 Hz, respectively.<sup>1</sup> Inflight performance of the spacecraft pointing control and stability achieved using both RWA and RCS thrusters are given in Refs. 1 and 5.

There are strong couplings between the thrust vector controller design (which is the responsibility of the GN&C team), selections of propellant tanks and PMD (which is the responsibility of the Propulsion team), and the placements of propellant tanks (which is the responsibility of the Structure team).<sup>2</sup> For example, the Cassini TVC (Thrust Vector Control) bandwidth, 0.23 Hz, was selected to be higher than the high-g slosh frequencies of the propellants at all tank fill fractions. During spacecraft thrusting maneuvers, the sloshing of liquid propellant in partially filled tanks can interact with the controlled system in such a way as to cause the overall system to be unstable. These propellant tanks must be properly placed, relative to the spacecraft’s c.m., to avoid any unstable interactions. For all these reasons, the GN&C, Propulsion, and Structure teams must collaborate closely during the design phase of the spacecraft. As of February 24, 2014, the Cassini spacecraft has performed 284  $\Delta V$  burns since launch on October 15, 1997. Of these, 163 burns have utilized the bi-propellant main engine while 121 burns have

used the hydrazine thrusters.

Propellant slosh oscillations and vibratory motions of structural booms triggered by the firing of the 445-N main engine will generate signatures that might be observable in selected S/C telemetry. Hence, telemetry data of these propulsive burns could be used to characterize the propellant slosh and structural boom frequencies. Results of these characterizations of the high-g propellant slosh frequencies are given in Section III. Upon the completion of a main engine burn, the high-g field generated by the 445-N engine thrust is “removed” and the high-g slosh modes damped out quickly. However, the vibratory motion of the magnetometer boom, triggered by the burn, will continue to interact with the S/C base-body. These interactions could be detected if one look at the power spectra of the telemetry data of the RWA control torque. In Section IV, the estimated frequency of the magnetometer boom is compared with that predicted analytically. Conclusions are given in Section V.

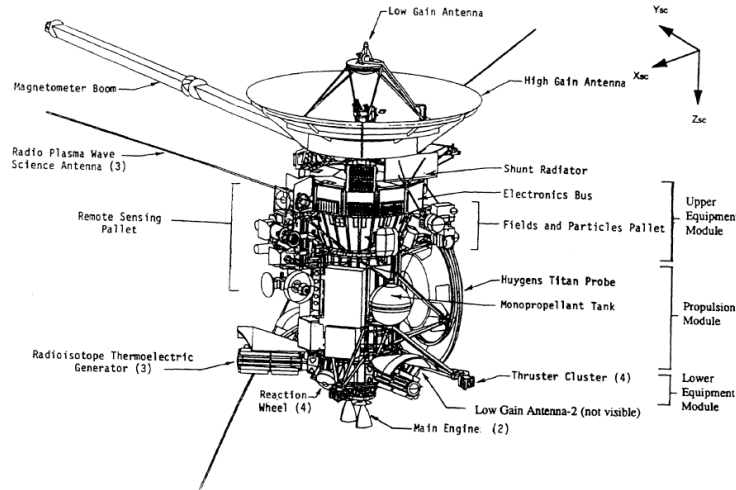


Figure 1. Cassini Spacecraft Cruise Configuration (from Ref. 1)

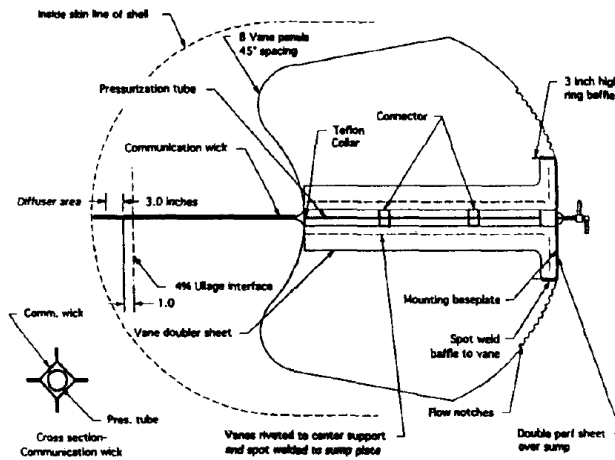


Figure 2. Cassini Propellant Management Device (from Ref. 4).

## II. Predictions of Cassini Bi-propellant Propellant Slosh Modes

At the time of launch, the Cassini spacecraft mass was 5,574 kg. Therefore, the axial acceleration of the spacecraft during rocket engine burns (with a nominal thrust of 445 N) in the early Cruise phase was about 0.09

m/s<sup>2</sup>. When the spacecraft experienced this “high” acceleration, the bi-propellant settled to the “bottom” of the tanks and assumed a “rough flat” surface that is perpendicular to the thrust vector of the engine. For the purpose of thrust vector control during a main engine burn, two gimbal actuators are used to articulate the main engine thrust. This introduces lateral acceleration disturbances. Propellant responds by forming standing waves on the “free” surface, which is called “sloshing”. In this “main engine firing” scenario, the sloshing motion of the bipropellant in the tanks is in a so-called “high-g” mode. A dimensionless parameter, the Bond number  $Bo$ , is defined by  $\rho a R^2 / \sigma$ . In this expression,  $\rho$  is the density of the liquid at 20 °C (870 and 1,450 kg/m<sup>3</sup> for MMH and NTO, respectively),  $\sigma$  is the surface tension parameter of the liquid at 20 °C (0.0343 and 0.0237 N/m for MMH and NTO, respectively), and  $R$  is the tank radius (0.62 m). It is the ratio of acceleration to surface tension forces. In general, propellant sloshing is in a “high-g” mode when the Bond number is  $>10$ .

When the spacecraft attitude is controlled by a set of three reaction wheels (RWA’s), the only relatively significant forces acting on the spacecraft are the centrifugal forces due to the static imbalances of the RWA. In this state, the bipropellant liquid is in a so-called “low-g” sloshing mode. In this mode, surface tension forces control the motion of the propellant inside the tanks. The propellant will assume a shape determined by surface tension forces and the geometry of PMD. When a S/C’s  $\Delta V$  is executed using a set of four monopropellant thrusters (with a nominal thrust of 1 N at the time of launch), the acceleration level experienced by the S/C is about 0.000723 m/s<sup>2</sup>. This is more than a factor of 100 lower than that experienced by the S/C during a main engine burn. Under these circumstances, the sloshing motions of the bipropellant in the tanks are also in a “low-g” mode.

Over the past decades, there have been numerous analytical approaches used to predict propellant slosh characteristics in spacecraft’s propellant tanks. Among those approaches are the methods described in a classic Apollo era NASA publication (SP-106<sup>6</sup>), an updated version of this same treatise by Southwest Research Institute,<sup>7</sup> and in many other publications such as Refs. 8–13. These references describe analytic techniques for estimating the four key slosh parameters (frequency, participatory mass, pendulum pivot location, and damping factor) for a variety of basic tank shapes including spherical and upright cylindrical. The frequencies and damping factors of high-g and low-g sloshing motions in Cassini bipropellant tanks are given in Refs. 9 and 10 (among others), and reported in Ref. 4. These results will be briefly reviewed in this section. Not included here are the details of their derivations, though they exist in the references.<sup>4,9–10</sup>

The Cassini propulsion module houses two identical cylindrical tanks with hemispherical end domes. The radius of the end domes is 0.62 m and the height of the cylindrical section is 0.32 m. Both geometric centers of these axisymmetric tanks are located on the S/C’s Z-axis. These tanks each contain an eight-panel PMD of the surface tension type. These PMDs are used to control the orientation of the propellant in the space environment (see Fig. 2). As explained in Ref. 4, the complex fluid motion in the tank (with PMD) could be approximated by two different high-g propellant slosh modes (two for liquid in each tank): The sector mode and the full-tank mode. The sector mode represents propellant motion that occurred inside the 45-deg sectors of the PMD. Based on theoretical and experimental works documented in Refs. 6–8, the sector frequency for a flat-bottomed 45-deg cylindrical tank is given approximately by  $0.312 \sqrt{a/R}$  Hz, where “a” is the acceleration and “R” is the radius of the sectored tank. See Appendix A for details. At a tank fill fraction of about 50%, with the mass of the spacecraft at 3,800 kg, an engine thrust of 445 N, and for a tank radius of 0.62 m, the predicted frequency is 0.139 Hz.

The full-tank mode may be understood with the help of another tank shape in which the fluid motion is confined between two concentric flat-bottomed cylinders. The inner cylinder can be regarded as a gross representation of the PMD. It was thought that the fundamental slosh mode for this type of tank would be somewhat similar to the way the fluid flows around the PMD in the Cassini tank. Using the 49.5 cm radius of the PMD vane, the inner-to-outer radius ratio is  $k = 49.5/62 \approx 0.8$ . With reference to Fig. 2.5 of Ref. 6, the fundamental frequency of slosh motion (it was called “full tank” propellant slosh mode in Ref. 6) is given by  $0.15 \sqrt{a/R}$  Hz.<sup>‡</sup> Again, “a” is the acceleration and “R” is the “outside” radius of the annular tank. At a tank fill fraction of about 50%, this full-tank slosh frequency is about 0.065 Hz. It was suspected that the spherical bottom end dome of the Cassini tank might cause the frequency of this mode to shift downward.<sup>4,18–19, 21–22</sup> Predicted high-g sector and full-tank mode frequencies for the Cassini tanks (with spherical end domes) are given in Refs. 9–10. These frequencies, as functions of tank fill fractions, are tabulated in Table 1.<sup>4,9</sup>

<sup>‡</sup>Actually, with reference to Fig. 2.5 of Ref. 6, the annular slosh frequency (for  $k=0.8$ ) should be given by  $0.162 \sqrt{a/R}$  Hz. But this is quoted as  $0.15 \sqrt{a/R}$  Hz in Ref. 4 (as a rounded approximation). In this paper, we will follow the relation quoted in Ref. 4. But see the discussion given near the end of Section III.

**Table 1. Cassini Bipropellant High-g Slosh Frequency<sup>4,9</sup>**

Tank Fill Fraction [%]	Acceleration [m/s <sup>2</sup> ]	Full-tank Mode Slosh Frequency* [Hz]	Sector Mode Slosh Frequency* [Hz]
0	0.266	-	-
20	0.190	0.031	0.168
40	0.139	0.044	0.148
50	0.127	0.046	0.142
60	0.117	0.049	0.136
80	0.101	0.078	0.131
100	0.089	-	-

\*The full-tank and sector mode slosh frequencies given in this table, as functions of the tank fill fraction and acceleration level, were based on results documented in Ref. 4 (Fig. 4 of Ref. 4). However, acceleration is related to both the engine thrust and the mass of the spacecraft at the time of engine thrusting. In Ref. 4 (published in 1994), the assumed thrust of the Cassini main engine was 490 N. The engine thrust was subsequently changed to 445 N. There was also a change in the spacecraft's mass (launch mass was assumed to be 5,300 kg in 1994 while actual launch mass was 5,574 kg). As a result of these changes, the fill fractions and accelerations given in this table do not correspond *exactly* to those of the actual spacecraft.

When the spacecraft attitude is controlled by a set of three reaction wheels (or the 1-N thrusters), the bipropellant is in a so-called “low-g” sloshing mode. In this mode, surface tension forces control the motion of the propellant inside the tanks. The prediction of the low-g slosh motion in the Cassini MMH/NTO tanks (with PMD) is very challenging. The procedure described in Ref. 10 that was used to predict Cassini low-g slosh motion is summarized in Ref. 4. In that procedure, the tool Surface Evolver described in Ref. 11 played a pivotal role. But simulation results from Surface Evolver alone is not adequate to predict the slosh frequencies and additional engineering judgments must be made in order to produce the final low-g propellant sloshing pendulum. The approach taken was to “guess” the pendulum length based on the graphical Evolver-based data, and then to derive other pendulum model parameters accordingly.<sup>4</sup> Results of the predicted low-g propellant slosh frequencies, as functions of tank fill fractions, are tabulated in Table 2.<sup>4,10</sup>

In this study, we have analyzed telemetry data obtained when the spacecraft was controlled by a set of reaction wheels. But since no clear low-g “signature” is detected in these data, the predicted low-g slosh frequencies given in Table 2 could not be confirmed. Low-g slosh motions, at frequencies of 3.3–6.9 mHz (see Table 2), are within the bandwidth of the RWA attitude controller (30 mHz).<sup>5</sup> Together with the fact that typically low-g slosh modes have damping ratios that are >10%, it was hard to detect them.

In Ref. 5, the time history of the Z-axis attitude control error of a thruster-based science observation made on 2008-DOY-004 exhibited a distinct behavior. It appeared that thrusters' firing have excited a particular spacecraft flexible mode with a frequency of 2.5 mHz (16 cycles in 1.8 hours). At the time of that science observation, the MMH/NTO tanks' fill fraction was about 13% and the predicted low-g slosh frequencies was analytically predicted to be 3–5 mHz (see Table 2). However, damping ratio of low-g slosh motion is predicted to be >10%<sup>4</sup> while the observed oscillation was un-damped over >1.8 hours. Also, the oscillatory motion was about the tank's axis of symmetry instead of its lateral axes. For these reasons, we have discounted it as a low-g slosh oscillation, and will not study it in this study. See Appendix B for details.

**Table 2. Cassini Bipropellant Low-g Slosh Frequency<sup>4,10</sup>**

Tank Fill Fraction [%]	NTO Slosh Frequency [mHz]	MMH* Slosh Frequency [mHz]
10	4.45	6.90
20	3.20	5.00
30	2.96	4.59
40	2.81	4.36
50	2.85	4.42
70	3.30	5.12

\*The MMH frequency can be obtained directly by multiplying the NTO slosh frequency by the square root of the ratio of kinematic surface tensions of MMH to NTO, which is 1.55.

The hydrazine tank of Cassini is spherical with a radius of 0.36 m and it includes an elastomeric diaphragm to deliver bubble-free hydrazine to the thruster lines. At the time of launch, the tank was 70% full with 132.1 kg of hydrazine. The polymeric rubber diaphragm was expected to increase both the damping and the “clean tank” slosh frequency. Based on experimental works recorded in Refs. 12–13, the high-g propellant slosh of the hydrazine propellant was estimated to be about 1.3 Hz with a 0.3 (30%) damping ratio.<sup>4</sup> Power spectra of telemetry data such as the per-axis spacecraft rate estimates will be used in Section III to characterize the slosh frequencies of the bi-propellant fuel and oxidizer. Typically, these telemetry data are available at 0.5 Hz or lower. Hence, characteristic frequencies that are above the Nyquist frequency of 0.25 Hz, such as the high-g monopropellant hydrazine could not be estimated via this approach. Overall, the relatively high damping and stiffness of the monopropellant fuel as well as its relative small mass made the characterization of monopropellant fuel motion of less important.

### III. Inflight Estimated Cassini Bi-propellant High-g Propellant Slosh Modes

Cassini, a three-axis stabilized orbiter, uses two-axis engine gimbal actuators for thrust vector control (TVC). During a burn of the 445-N engine, the X and Y-axis of the spacecraft’s attitude are controlled by the gimbal actuators using a TVC algorithm.<sup>1</sup> At the same time, four Y-facing thrusters are used to control the spacecraft’s Z-axis motion. As of February 24, 2014, the Cassini spacecraft has performed 284  $\Delta V$  burns since launch on October 15, 1997. Of these, 163 burns have utilized the bi-propellant main engine while 121 burns have used the monopropellant thrusters. Propellant slosh oscillations triggered by the firing of the 445-N main engine will generate signatures that might be observable in selected S/C telemetry both during the burn. Hence, telemetry data of these propulsive burns could be used to characterize the propellant slosh frequencies. A similar approach was used to estimate the liquid slosh frequencies in the propellant tank of the Mars Reconnaissance Orbiter.<sup>17</sup>

The power spectral density of the spacecraft’s X-axis angular rate during the first few minutes of the Deep Space Maneuver (DSM) is depicted in Fig. 3. Its counterparts for two other large burns, Saturn Orbit Insertion (SOI) and the Periapsis Raise Maneuver (PRM) are given in Figures 4 and 5, respectively. In this study on the inflight characterization of propellant sloshing, we focused on flight data collected in the first 4.233 minutes (4.233 min. is  $254 \text{ sec} = 2^8 - 2 \text{ sec}$  where the telemetry sampling time is 2 sec) after burn start. Propellant slosh motion is relatively more pronounced (and more observable) in this time window before PMD damping and thrust vector control actions suppressed them.

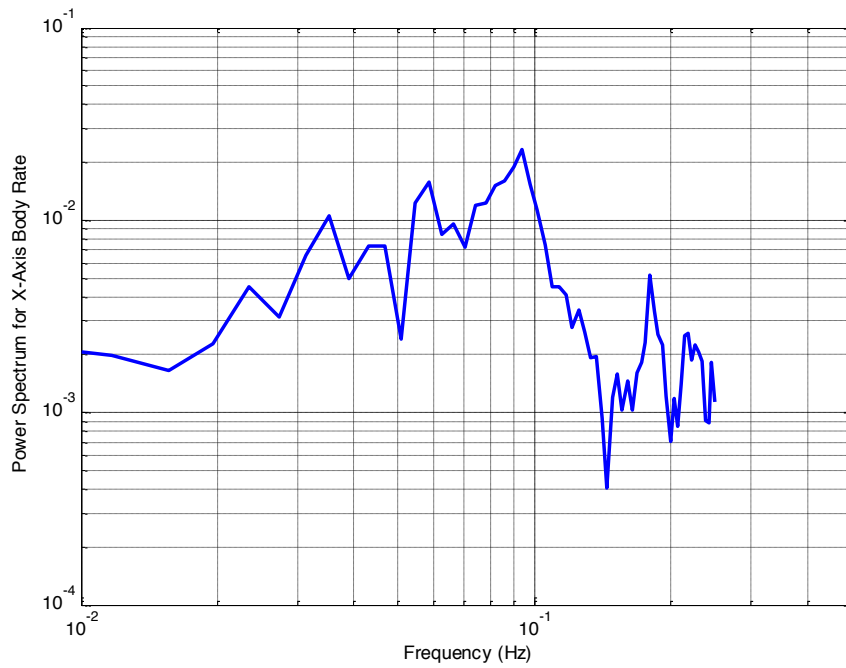


**Figure 3. Power Spectral Density of the Spacecraft's X-axis Rate During DSM**

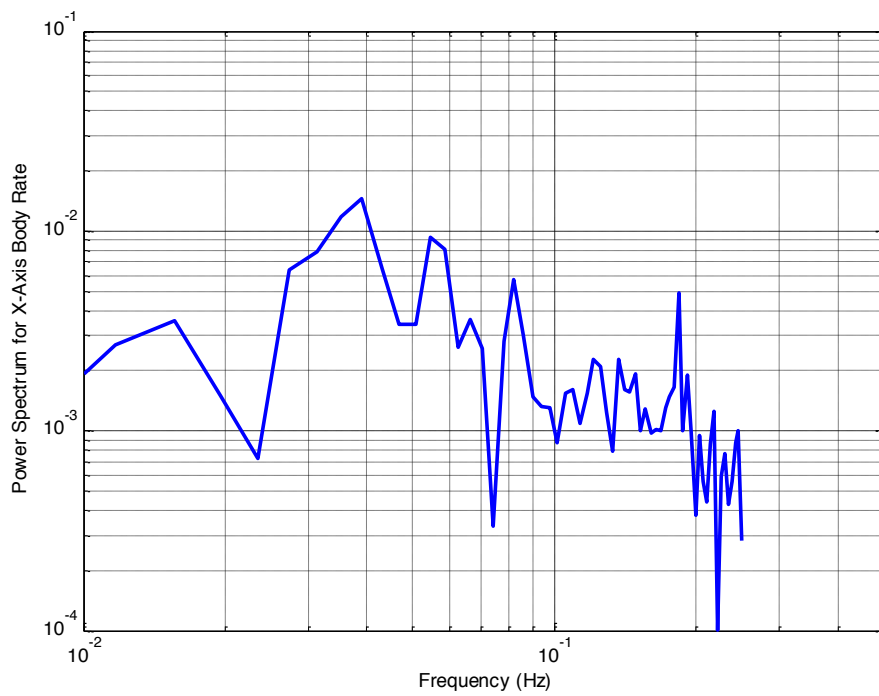


**Figure 4. Power Spectral Density of the Spacecraft's X-axis Rate During SOI**

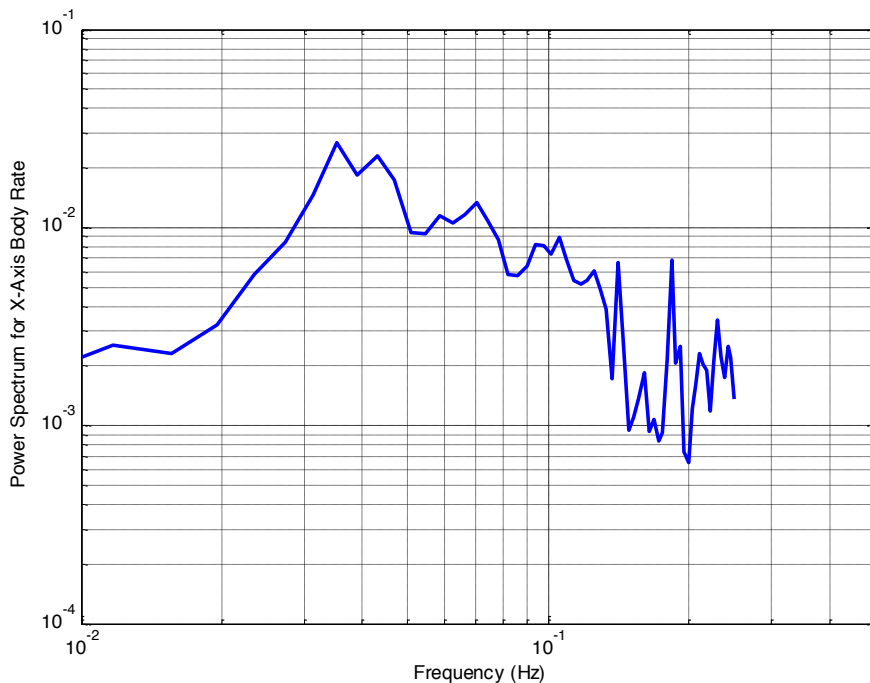


**Figure 5. Power Spectral Density of the Spacecraft's X-axis Rate During PRM**

Stable limit cycles with frequencies of about 0.03-0.04 Hz were observed in all “dynamics”-related telemetry (for example, spacecraft’s per-axis angular rates, engine gimbals angles, etc.) of all “long” burns performed with a rocket engine.<sup>1</sup> These limit cycles were first observed in the telemetry of the Deep Space Maneuver performed in 1998. They were also observed during the long Saturn Orbit Insertion burn executed in 2004. The frequencies of these limit cycles were about 0.035 Hz near the start of the DSM burn (see Fig. 3). The frequencies observed near the start of the SOI and PRM burn were 0.039 and 0.035–0.043 Hz, respectively (see Figs. 4 and 5). The observed limit cycle frequency is quite close to the high-g full-tank slosh frequency reported in Ref. 4 (see Table 1). However, as explained in Ref. 1, what we observed wasn’t the slosh frequency. Instead, the source of the observed sustained oscillation in the S/C’s rates came from a stable interaction between nonlinear elements of the engine gimbal actuators (e.g., actuator backlash) and the thrust vector control algorithm. See Ref. 1 for details.

Guided by predicted frequency ranges of the full-tank and sector propellant slosh modes tabulated in Table 1, observed peaks in Figs. 3–5 are tabulated in Table 3. For a flat-bottomed 45° sector tank, the high-g sector frequency for an engine burn is estimated to be  $0.312 \sqrt{a/R}$  Hz.<sup>4,6-8,20</sup> See Appendix A for details. For the SOI burn, the acceleration ( $a$ ) is 0.0984 m/s<sup>2</sup>,  $R$  is 0.62 m, and hence the predicted sector frequencies are 0.124 Hz. There are three observed peaks (0.109, 0.121, and 0.137 Hz) in Fig. 4. Apparently, the complex and numerous interactions involved with liquid sloshing in a 45° compartmented tank resulted in multiple sector propellant slosh modes. The predicted frequency (0.124 Hz) is close to the mid-point of the three observed peaks (which is 0.122 Hz). The frequency estimation formula given above is only applicable for a flat-bottomed tank with 45° sectors that run the entire length of the tank. But the panels of the Cassini PMD extend to the tank wall only at the bottom, and they do not run the entire height of the tank (see Fig. 2). Also, the ends of the Cassini tank are not flat, but have spherical caps. Nonetheless it was conjectured that the PMD panels would compartment the fluid enough so that a mode similar to the 45° sector mode would appear, and that the frequency would be close to the flat-bottomed frequency, at least for medium fill levels where the mode is assumed insensitive to the exact shape of the tank bottom. These conjectures are confirmed by the SOI results of this study. The prediction error of the sector mode slosh frequency is on the order of 5–6%.

<sup>1</sup> The fill fraction at SOI was about 60% (see Table 3). From Table 1, the estimated acceleration was 0.117 m/s<sup>2</sup> and the corresponding sector frequency was 0.136 Hz (in Ref. 4, 1994). The actual SOI acceleration was 0.0984 m/s<sup>2</sup>, and hence the revised sector frequency is  $0.136 \times (0.0984/0.117)^{0.5} \approx 0.1247$  Hz. This is consistent with that computed using the formula.

**Table 3. Cassini Bipropellant Observed Frequencies for Three Large Main Engine Burns**

Burn	Date	Burn Time [min]	Burn Start Fill Fraction [%]	Sector Mode		Full Tank Mode	
				Predicted [Hz]	Observed [Hz]	Predicted [Hz]	Observed [Hz]
DSM	12/3/98	86.9	93	*	*	0.077 (1 <sup>st</sup> ) 0.130 (2 <sup>nd</sup> )	0.059–0.094 0.125
SOI	7/1/04	97.4	61	0.124 (1 <sup>st</sup> ) 0.146 (2 <sup>nd</sup> )	0.109–0.137	0.0697	0.055–0.082
PRM	8/23/04	50.9	35	0.138 (1 <sup>st</sup> ) 0.162 (2 <sup>nd</sup> )	0.125–0.141	0.077	0.059–0.106

\*The Cassini PMD is completely submerged by the liquid at this fill fraction. In this condition, the sector mode disappeared. The full-tank mode frequency should approach that of a “clean tank”.

That the analytically predicted magnitude of the sector slosh frequency matches quite well the observed frequency is somewhat of a surprise. Because it is well known that analytically predicted slosh frequency only agrees with experimental results when the excitation amplitude of the liquid is small,<sup>4,6–8,20</sup> it was expected that the analytical slosh sector frequencies would not be an accurate prediction of observed frequencies. High amplitude slosh excitation will cause a drop in the slosh frequency in both compartmented and un-compartmented tanks. Our conjecture is that the 45°-sector of the Cassini PMD has added a significant amount of damping to the system to ensure that only small amplitude liquid motions are generated.

Using a similar approach, the predicted sector mode slosh frequency at the start of the PRM burn is 0.138 Hz. This predicted sector frequency is close to but higher than the mid-point of the two observed peaks (0.109 and 0.141 Hz), which is 0.125 Hz. This is not a surprise because at the time of the PRM burn, all the liquid was in the spherical end dome of the tank (see Figure A2 of Appendix A). The sloshing liquid motion in the tank at low PRM fill fractions is not well modeled by the “superposition” of a sector mode and a full-tank mode. At low fill fraction, the stand-pipe in the center of the baffle assembly tends to be filled with liquid under the action of surface tension (as per design). As such, significantly more liquid will stay within the stand-pipe instead of the 45° sectors. Based on the PRM results, the over-prediction factor is about  $0.138/0.125 = 1.1$ .

The fill fractions of the tanks at the start of the DSM burn were 93%. At this fill level, the PMD was completely submerged by the liquid. Hence, the sector mode should have disappeared and only the full-tank mode remained. The full-tank mode frequency should approach that of a “clean tank” (i.e., un-compartmented tank). From Table 1 of Ref. 20, the theoretical bare-wall clean cylindrical tank slosh frequency is given by  $\omega^2 R/a = 1.84$  (see also Appendix A). The acceleration at the start of DSM is  $0.0798 \text{ m/s}^2$ . With  $R = 0.62 \text{ m}$ , the fundamental frequency of propellant slosh motion in a “clean” tank is 0.077 Hz. From Fig. 3, we observed three peaks at frequencies of 0.059, 0.094, and 0.125 Hz. The predicted clean-tank frequency is close to the mid-point of the peaked frequencies at 0.059 and 0.094 Hz (which is 0.076 Hz). Apparently, the presence of the submerged PMD structure “splits” the clean-tank frequency from one into two modes with frequencies that are slightly higher and lower than the predicted frequency. The predicted 2<sup>nd</sup> clean-tank frequency (0.130 Hz) is close to the peaked frequency at 0.125 Hz.

The high-g *full-tank* propellant slosh mode at the SOI fill fraction is analyzed next. The full-tank mode may be understood with the help of another tank shape in which the fluid motion is confined between two concentric flat-bottomed cylinders ( $k$  is defined as the ratio of inside to outside diameter,  $k < 1$ ). The inner cylinder can be regarded as a gross representation of the PMD. It was thought that the fundamental slosh mode for this type of tank would be somewhat similar to the way the fluid flows around the PMD in the Cassini tank. There is a range of peaks observed at frequencies of 0.055, 0.066, and 0.082 Hz in Fig. 4. Apparently, the complex fluid motion associated with the full-tank mode could only be modeled by a combination of several modes. This might explain why a series of “peaks” are observed in Fig. 4.

The high-g full-tank mode frequency for a *flat-bottom* cylindrical tank, is estimated to be  $0.15 \sqrt{a/R}$  Hz.<sup>4,6–8</sup> Alternative estimates given in Ref. 20 are  $0.175 \sqrt{a/R}$  Hz and  $0.215 \sqrt{a/R}$  Hz for annular tanks with  $k$  of 0.8 and 0.5, respectively. For the SOI burn, the estimated full-tank frequencies are 0.0598 Hz (based on Ref. 4), 0.0697 Hz ( $k = 0.8$ ), and 0.086 Hz ( $k = 0.5$ ). This range of estimated frequencies is comparable to the observed frequency range of 0.055–0.082 Hz (see Fig. 4). The frequency predicted with  $k = 0.8$  seemed to match the mid-point of the observed peak frequencies (0.0685 Hz) the best. For the PRM burn, the estimated full-tank frequencies are 0.066 Hz (based on Ref. 4), 0.077 Hz ( $k = 0.8$ ), and 0.095 Hz ( $k = 0.5$ ). This range of estimated frequencies is comparable with the

observed frequency range of 0.059–0.106 Hz (see Fig. 5). Again, the frequency predicted with  $k = 0.8$  seemed to match the mid-point (0.0825 Hz) of the observed peak frequencies the best.

The last observed peak in Figs. 4 and 5 is near 0.183 Hz. It could be a 2<sup>nd</sup> sector propellant slosh mode or an aliased frequency of the magnetometer boom. Knowing that the magnetometer boom frequency is on the order of 0.67 Hz and the spacecraft rate telemetry was sampled only at 0.5 Hz (which is lower than twice the frequency of the magnetometer boom, or  $2 \times 0.67 = 1.34$  Hz), one can expect the occurrence of aliased data in the spectrum. Indeed, our analyses indicate that oscillatory motions of a 0.683-Hz magnetometer boom when sampled at 0.5 Hz will exhibit an aliased frequency of about 0.183 Hz. This estimated magnetometer boom frequency (made based on the aliased frequency of 0.183 Hz), 0.683 Hz, is indeed very close to the ground-based estimated frequency of the magnetometer boom, which is 0.691 Hz. See Section IV for further discussions on the inflight estimation of the magnetometer boom frequency.

#### IV. Modeling and Inflight Characterization of the Cassini Magnetometer Boom Frequency

The Cassini magnetometer has been designed and built specifically for measurements within the Saturnian environment.<sup>14</sup> Previous planetary flybys have shown the existence of an internal Saturn magnetic field, a magnetosphere, and a strong plasma interaction between Titan and its plasma surroundings. By measuring the magnetic field, which originates deep inside the planet, the magnetometer will provide information on conditions in and near the dynamo region. However, the magnetometer probes not only the deep interior of the planet (where the internal planetary field originates), but it also makes detailed measurements of the planetary environment, its magnetosphere and ionosphere, and those of the Saturnian moons.

On the magnetometer boom depicted in Fig. 1, the FGM (Flux Gate Magnetometer) sensor is mounted partway along the magnetometer boom, and the V/SHM (Vector/Scalar Helium Magnetometer) sensor is mounted at the tip of the magnetometer boom. The Cassini magnetometer boom may be modeled as a cantilever beam with length  $L$  m and two concentrated masses, one representing the FGM sensor ( $M_1$  kg) and the other one for the V/SHM sensor ( $M_2$  kg). The mass representing the FGM sensor is located at  $AL$  m (i.e.,  $M_1$  is located at a fraction  $A$  of the full length,  $L$ ). The mass of the boom is uniformly distributed with a linear “density” of  $\rho$  (in kg/m). The Young modulus ( $E$ ) and area moment of inertia ( $I$ ) of the magnetometer boom is  $EI$ . Estimated magnitudes of these parameters are:  $M_1 = 5.22$  kg,  $M_2 = 2.41$  kg,  $A = 0.4627$ ,  $EI = 2.6e4$  N-m<sup>2</sup>,  $L = 9.378$  m, and  $\rho = 1.337$  kg/m.

The exact solution of cantilever vibration problems involving continuous system is often laborious, and the required calculations are frequently prohibitive. Approximate solutions for the fundamental frequency of various structures are available and often time they yield results with good accuracy. Of the many methods available in the literature for the determination of frequency, the Rayleigh’s energy method is the most commonly used one.<sup>15</sup> To use this method, we first determine the static deflection ( $y$  in Eq. (1)) of the cantilever beam under its own weight and the two concentrated masses:

For  $0 \leq x \leq AL$

$$\frac{EI}{gL^3} y(x) = \frac{1}{2} (AM_1 + M_2 + \frac{\rho L}{2}) \left(\frac{x}{L}\right)^2 - \left(\frac{M_1 + M_2 + \rho L}{6}\right) \left(\frac{x}{L}\right)^3 + \left(\frac{\rho L}{24}\right) \left(\frac{x}{L}\right)^4$$

Deflection at  $x = AL$ :

$$\frac{EI}{gL^3} y_{\text{midspan}} = \frac{A^3}{3} M_1 + \left(\frac{A^2}{2} - \frac{A^3}{6}\right) M_2 + \left(\frac{A^2}{4} - \frac{A^3}{6} + \frac{A^4}{24}\right) \rho L = G_1 \text{ (by definition)}$$

For  $AL \leq x \leq L$

$$\frac{EI}{gL^3} y(x) = -\frac{A^3}{6} M_1 + \frac{A^2}{2} M_1 \left(\frac{x}{L}\right) + \left(\frac{M_2 + \rho L}{2} + \frac{\rho L}{4}\right) \left(\frac{x}{L}\right)^2 - \left(\frac{M_2 + \rho L}{6}\right) \left(\frac{x}{L}\right)^3 + \left(\frac{\rho L}{24}\right) \left(\frac{x}{L}\right)^4 \quad (1)$$

Deflection at tip of boom ( $x = L$ ):

$$\frac{EI}{gL^3} y_{\text{max}} = \left(\frac{A^2}{2} - \frac{A^3}{6}\right) M_1 + \frac{M_2}{3} + \frac{\rho L}{8} = G_2 \text{ (by definition)}$$

To estimate the natural frequency of the boom, one equates the maximum potential energy of the system to the maximum kinetic energy. The natural frequency of the magnetometer boom ( $\Omega$ ) is given by Eq. (2):

$$\Omega^2 \approx \frac{g \sum_{i=1}^2 M_i y_i + \int_0^L \rho g \delta(x) dx}{\sum_{i=1}^2 M_i y_i^2 + \int_0^L \rho \delta^2(x) dx} \quad (2)$$

where  $y_1 = y_{\text{mispan}}$  and  $y_2 = y_{\text{max}}$  given in Eq. (2)

In Eq. (2),  $\delta(x)$  is the approximate form of static deflection ( $y(x)$ ) of the cantilever beam given in Eq. (1). For simplicity, we will approximate it using a parabola (instead of using the 4<sup>th</sup> order polynomial relations given in Eq. (1)):

$$\begin{aligned} \delta(x) &\approx y_{\text{max}} \left(\frac{x}{L}\right)^2 \\ \int_0^L \rho g \delta(x) dx &= \frac{1}{3} \rho g y_{\text{max}} L \\ \int_0^L \rho \delta^2(x) dx &= \frac{1}{5} \rho y_{\text{max}}^2 L \\ \Omega^2 &= \frac{g \sum_{i=1}^2 M_i y_i + \frac{1}{3} \rho g y_{\text{max}} L}{\sum_{i=1}^2 M_i y_i^2 + \frac{1}{5} \rho y_{\text{max}}^2 L} = \left(\frac{EI}{L^3}\right) \frac{M_1 G_1 + (M_2 + \frac{\rho L}{3}) G_2}{M_1 G_1^2 + (M_2 + \frac{\rho L}{5}) G_2^2} \end{aligned} \quad (3)$$

Based on the estimated values of  $M_1$ ,  $M_2$ ,  $A$ ,  $EI$ ,  $L$ , and  $\rho$ , the estimated frequency of the magnetometer boom is 0.6522 Hz. The most accurate ground-based estimated frequency of the magnetometer boom produced 0.6909 Hz.<sup>16</sup> The Rayleigh's energy method produced a frequency estimate that is within 5.6% of the measured value. The modal damping ratio of the magnetometer boom is about 1%.

The fundamental frequency of the three RPWS antennas could be estimated similarly. For the RPWS antenna, there aren't any concentrated masses located at either the mid-span or the end of the boom. That is,  $M_1 = M_2 = 0$  kg, and the mass density of the antenna is  $\rho = 0.1$  kg/m. The  $EI$  and  $L$  of the RPWS are  $53 \text{ Nm}^2$  and  $10$  m, respectively. Substitutions of  $M_1 = M_2 = 0$  kg in Eq. (3), the RPWS frequency is given by:

$$\Omega_{\text{RPWS}}^2 = \frac{40}{3} \left(\frac{EI}{\rho L^4}\right) \quad (4)$$

The estimated value of the fundamental frequency of the RPWS antennas is 0.134 Hz. The predicted frequency agrees quite well with that measured, which is 0.175 Hz. The modal damping ratio of the RPWS antennas is about 0.2%. Since the three RPWS antennas are identical in mass properties (only their orientations are different), there should be a total of six modes at this frequency (one in-plane and one out-of-plane for each of the three RPWS antennas).

During the early phase of Cassini cruise to Saturn, thrusters were used to roll and yaw the spacecraft attitude so as to align the pre-aimed rocket engine with the target  $\Delta V$  vector.<sup>1</sup> This thruster-based slewing imparts unwanted  $\Delta V$  on the spacecraft. Even though the magnitudes of these  $\Delta V$  could be predicted, they still, in a small way, affect the accuracy of the burn. As such, beginning with TCM-18 (Trajectory Correction Maneuver), both the roll and un-roll turns were executed using the reaction wheels. These RWA-based slews do not produce unwanted  $\Delta V$  and also saves hydrazine.

During a ME burn, both the high-g propellant slosh modes and the flexible appendages (RPWS antennas and the magnetometer boom) are excited. Once the burn is terminated, the high-g field generated by the 445-N engine thrust is "removed" and the high-g slosh modes damped out quickly. However, the vibratory magnetometer boom will continue to interact with the S/C base-body even when control is transitioned from thrusters to reaction wheels. Since the mass of the RPWS antennas is small relative to that of the magnetometer boom (mass of each RPWS antenna is 1 kg, which is <5% of the mass of the magnetometer boom), vibratory motions of the RPWS antennas made an insignificant contribution to these appendage/spacecraft interactions. These interactions could be detected if one compares the power spectra of the telemetry data of the RWA-1 (or the other two active RWAs) command torque, before and after the main engine burn. The power spectra that correspond to OTM-21 burn (5.833 m/s that lasted 37.35 s and was executed on April 10, 2005) are depicted in Fig. 6.

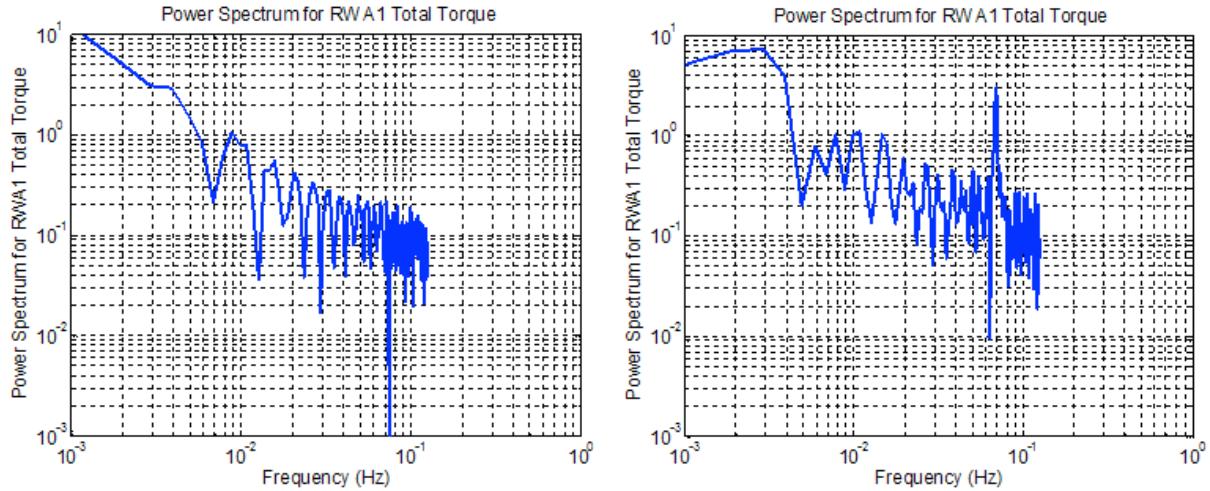


**Figure 6. Power Spectra of RWA-1 Torque Before and After A Main Engine Burn**

A comparison between the “before burn” and “after burn” power spectra showed a clear power spectrum spike at a frequency of 0.06836 Hz in the post-burn data. Knowing that the magnetometer boom frequency is on the order of 0.67 Hz and the RWA-1 torque telemetry was sampled only at 0.25 Hz (which is lower than twice the frequency of the magnetometer boom, or  $2 \times 0.67 = 1.34$  Hz), one can expect the occurrence of aliased data in the post-burn power spectrum. Indeed, our analyses indicate that oscillatory motions of a 0.6816-Hz magnetometer boom when sampled at 0.25 Hz will exhibit an aliased frequency of about 0.06836 Hz. This estimated magnetometer boom frequency (made based on the aliased frequency of 0.06836 Hz), 0.6816 Hz, is indeed very close (about 1% lower) to the ground-based estimated frequency of the magnetometer boom, which is 0.6909 Hz.<sup>16</sup> Actually, the estimated frequency is the damped frequency of the magnetometer boom,  $\Omega_n \sqrt{1 - \xi^2}$  where  $\xi$  is the damping factor of the boom. But since the estimated value of the damping factor is on the order of 1%, the damped frequency and the natural frequency of the boom are almost identical. Aliased frequencies that are very close to 0.06836 Hz were also observed in the power spectra of other spacecraft telemetry data such as the X-axis rate of the spacecraft. Post-burn telemetry data collected after other main engine burns (across a range of tank fill fractions) exhibited similar oscillatory motions of the magnetometer boom.

## V. Summary and Conclusions

About 55% of the total mass of the Cassini spacecraft at launch was bi-propellant. Hence, pre-launch, the Cassini attitude control design team paid special attention to the impact the sloshing liquid might have on controlling the spacecraft attitude in various phases of the Cassini mission. There are strong couplings between the thrust vector controller design (which is the responsibility of the GN&C team), sizing of the propellant tanks and PMD (which is the responsibility of the Propulsion team), and tank placements (which is the responsibility of the Structure team). During the design phases, the Cassini GN&C, Propulsion, and Structure teams collaborated closely in order to meet all propulsive maneuver execution accuracies. Analyses of the past 17 years of flight data indicate that all propellant sloshing-related issues (e.g., thrust vector control stability and spacecraft pointing stability during science observations) are addressed adequately.

A combination of low telemetry sampling rate and the effectiveness of the PMD make characterization of both high-g and low-g propellant sloshing challenging. For events where propellant sloshing is presumed observable, the accuracy of the analytical prediction varies. Overall, based on our limited-scope analyses of data from three major burns of the Cassini spacecraft, we conclude that the methodologies described in Ref. 4 have provided good prediction of the high-g *sector* mode slosh frequency. This is the case in spite of the fact that the prediction is made for a flat-bottomed 45° sectored tank while the Cassini tanks are not flat, but have spherical end caps. The prediction error of the sector mode slosh frequency is on the order of 5–6%. However, at lower tank’s fill fractions (e.g., at the start of the PRM burn when the fill fraction was 35%), when most of the liquid is in the spherical end dome, the prediction error deteriorated to >10%. Analytical formulae given in Ref. 20 (for flat-bottomed annular tanks with  $k = 0.8$ ) seem to be able to make accurate prediction of Cassini “*full-tank*” slosh frequency. Prediction error is on the

order of a few percent at fill fraction of about 60%. Again, at lower tank's fill fractions, the prediction error deteriorated to >10%.

For events where the structural frequencies of the magnetometer boom are observable, the observed structural frequency matches closely with both analytical predictions and ground measurement. The deviation between the predicted/measured and observed magnetometer frequencies is on the order of 1–4.3%. The pre-launch analytically predicted and measured structural frequencies of the magnetometer boom are confirmed.

### Acknowledgments

The work described in this paper was carried out by the Jet Propulsion Laboratory, California Institute of Technology, under contract with the National Aeronautics and Space Administration. Reference to any specific commercial product, process, or service by trade name, trademark, manufacturer, or otherwise, does not constitute or imply its endorsement by the United States Government or the Jet Propulsion Laboratory, California Institute of Technology. We wish to thank both Glenn Macala and Sima Lisman, senior members of the Guidance and Control section of JPL, for their review of an earlier version of this paper. Any remaining errors of fact or interpretation are of course the responsibility of the authors.

### References

<sup>1</sup>Lee, Allan Y. and Hanover, Gene, "Cassini Spacecraft Attitude Control System Flight Performance," Paper AIAA-2005-6269, *Proceedings of the AIAA Guidance, Navigation, and Control Conference, and Exhibit*, San Francisco, CA, Aug. 15–18, 2005.

<sup>2</sup>Lee, Allan Y., Alan Strahan, Rebekah Tanimoto, and Arturo Casillas, "Preliminary Characterization of the Altair Lunar Lander SLOSH Dynamics and Some Implications for the Thrust Vector Control Design," AIAA-2010-7721, *Proceedings of the AIAA Guidance, Navigation, and Control Conference*, August 2–5, Toronto, Ontario, Canada, 2010.

<sup>3</sup>Smith, K.S. and Peng, Chia-Yen, "Modal Test of the Cassini Spacecraft," *Proceedings of the 1997 IMAC XV - 15<sup>th</sup> International Modal Analysis Conference*, Orlando, Florida, USA, 1997.

<sup>4</sup>Enright, P. and Wong, E.C., "Propellant SLOSHING Models for the Cassini Spacecraft," AIAA Paper 94-3730, 1994.

<sup>5</sup>Pilinski, E. and Lee, A.Y., "Pointing Stability Performance of the Cassini Spacecraft," *Journal of Spacecraft and Rockets*, Volume 46, No. 5, September-October, 2009, pp. 1007–1015.

<sup>6</sup>Abramson, H.N., editor, NASA SP-106 "The Dynamic Behavior of Liquids in Moving Containers," 1966.

<sup>7</sup>Dodge, F. T., "The New "Dynamic Behavior of Liquids in Moving Containers," Southwest Research Institute, San Antonio, Texas, 2000 (this is an update of NASA SP-106 whose original authors are Norm Abramson, Douglas Michel, George Brooks, and Helmut Bauer).

<sup>8</sup>Abramson, H.N. and Garza, L.R., "Liquid Frequencies and Damping in Compartmented Cylindrical Tanks," *Journal of Spacecraft and Rockets*, Vol. 2, No. 3, pp. 453–455, May–June 1965.

<sup>9</sup>Dodge, F.T., and S.T. Green, "Propellant Motion Models for the CRAF/Cassini Spacecraft," Southwest Research Institute Project 04-4262, Contract 959045, March 1992.

<sup>10</sup>Tegart, J., "Analysis Task Report, Low-g SLOSH Analysis," CPMS-SM-001, August 1993.

<sup>11</sup>Tegart, J., "Three-dimensional Liquid Interfaces In Cylindrical Containers," AIAA-91-2174, AIAA/SAE/ASME/ASEE, 27<sup>th</sup> Joint Propulsion Conference, Sacramento, CA, June 24-26, 1991.

<sup>12</sup>Stofan, A.J. and Pavli, A.J., "Experimental Damping of Liquid Oscillations in A Spherical Tank by Positive Expulsion Bags and Diaphragms," NASA TN D-1311, Lewis Research Center, July 1962.

<sup>13</sup>Stofan, A.J. and Sumner, A.E., "Experimental Investigation of the SLOSH-DAMPING Effectiveness of Positive Expulsion Bags and Diaphragms in Spherical Tanks," NASA TN D-1712, Lewis Research Center, June 1963.

<sup>14</sup>Dougherty, M.K., Kellock, S., Southwood, D.J., Balogh, A., Smith, E.J., Tsurutani, B.T., Gerlach, B., Glassmeier, K.H., Gleim, F., Russell, C.T., Erdos, G., Neubauer, F.M., and Cowley, W.H., "The Cassini Magnetic Field Investigation," *Space Science Reviews* 114: 331–383, 2004.

<sup>15</sup>Hansen, H.M. and Chenea, P.F., "Mechanics of Vibration," John Wiley and Sons, Inc., New York, 1952.

<sup>16</sup>Norton, R.L., "Revised Cassini Magnetometer Boom Frequency Sensitivity Analysis," Jet Propulsion Laboratory, IOM 3541-94-228 dated November 9, 1994.

<sup>17</sup>Chapel, J.D., Schmitz, E., Sidney, W.P., Johnson, M.A., Good, P.G., Wynn, J.A., and Bayer, T., "Attitude Control Performance for MRO Aero-braking and the Initial Science Phase," Paper AAS-07-097, 30<sup>th</sup>, Rocky Mountain Guidance and Control Conference, 2007.

<sup>18</sup>Concus, P., Crane, G., and Satterlee, H., "Small Amplitude Lateral Sloshing in a Cylindrical Tank With a Hemispherical Bottom Under Low Gravitational Conditions," NASA CR-54700, 1967.

<sup>19</sup>Abramson, H.N. and Ransleben, G.E., "Some Comparison of Sloshing Behavior in Cylindrical Tanks With Flat and Conical Bottoms," ARS Journal, pp. 542-544, April 1961.

<sup>20</sup>Abramson, H.N. Garza, L.R. and Kana, D. D., "Liquid Sloshing in Compartmented Cylindrical Tanks," ARS Journal, pp. 978-980, June 1962.

<sup>21</sup>Salzman, J., and Mascia, W., 1969, Lateral Sloshing in Cylinders Under Low Gravitational Conditions, NASA TN D-5058.

<sup>22</sup>Labus, T., "Natural Frequency of Liquids in Annular Cylinders Under Low Gravitational Conditions," NASA TN D-5412, 1969.

**Appendix A**  
**Theoretical Predictions of High-g Liquid Sloshing Frequencies In**  
**Un-compartmented and 45° Sector Compartmented Cylindrical Tanks**

The natural frequencies of liquid slosh in an un-compartmented and a 45° sector compartmented tank have been documented in numerous past studies. See, for example, Refs. 6–8, 19, and 20. Results are given by the following expression:

$$\frac{\omega_n^2 R}{a} = \lambda \tanh\left(\lambda \frac{h}{R}\right) \quad (\text{A1})$$

In this expression,  $\omega_n$  is the natural frequency of the liquid slosh motion in rad/s,  $R$  is the radius of the cylindrical tank, “ $a$ ” is the axial acceleration in  $\text{m/s}^2$ ,  $h$  is the depth of the liquid in the tank in m (see Fig. A1), and  $\lambda$  is a dimensionless eigen-value frequency parameter predicted in the above cited references.

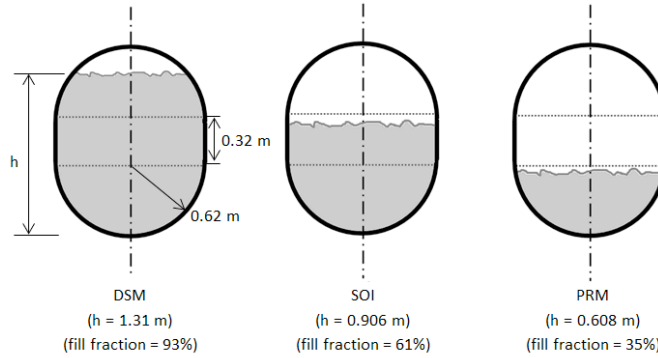


**Figure A1. Liquid Depths in Tanks before Ignition of the DSM, SOI, and PRM Burns**

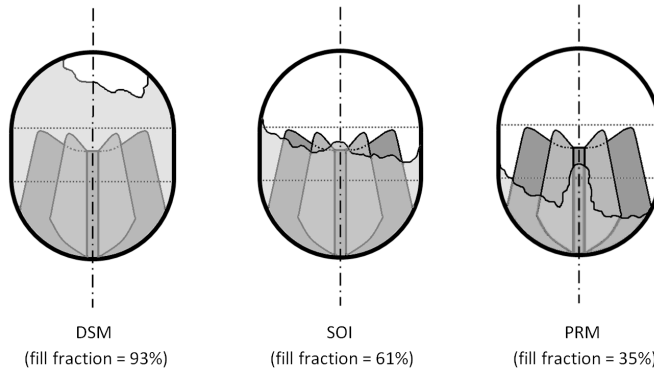


**Figure A2. Liquid Motions in Tanks at Starts of the DSM, SOI, and PRM Burns**

(In Figure A1, the liquid surfaces are shown perpendicular to the tank axis. In reality, the engine thrust vector is tilted  $\approx 7^\circ$  from the tank axis)

At the start of the DSM burn, the fill fractions of the tanks are 93%. The corresponding liquid depth is 1.31 m ( $h/R = 2.113$ ). At this fill level, the PMD was completely submerged by the liquid. Hence, the sector propellant slosh mode should have disappeared and only the full-tank mode remained. The full-tank mode frequency should approach that of a “clean tank” (i.e., un-compartmented tank). The  $\lambda$  for the 1<sup>st</sup> and 2<sup>nd</sup> mode of the clean tank slosh frequencies are 1.84 (1<sup>st</sup> mode) and 5.33 (2<sup>nd</sup> mode). Since  $\tanh(1.84 \times 2.113) \approx \tanh(3.888) \approx 0.99916$ , and  $\tanh(5.33 \times 2.113) \approx \tanh(11.26) \approx 1.00000$ , we have the following approximate expressions for the first two slosh frequency modes of the un-compartmented tank:

$$\omega_1^{\text{uncompartment}} = 0.216 \sqrt{\frac{a}{R}} \text{ Hz}, \quad \omega_2^{\text{uncompartment}} = 0.367 \sqrt{\frac{a}{R}} \text{ Hz}. \quad (\text{A2})$$

At the start of the SOI burn, the fill fractions of the tanks are 61%. The corresponding liquid depth is 0.906 m ( $h/R = 1.46$ ). The  $\lambda$  for the 1<sup>st</sup> and 2<sup>nd</sup> mode of the sector slosh frequencies are 3.84 and 5.29, respectively. Since

$\tanh(3.84 \times 1.46) \approx \tanh(5.606) \approx 0.999973$ , and  $\tanh(5.29 \times 1.46) \approx \tanh(7.723) \approx 0.999999$ , we have the following approximate expressions for the sector slosh frequencies of a  $45^\circ$  compartmented tank:

$$\omega_1^{\text{compart}} = 0.312 \sqrt{\frac{a}{R}} \text{ Hz}, \quad \omega_2^{\text{compart}} = 0.366 \sqrt{\frac{a}{R}} \text{ Hz} \quad (\text{A3})$$

The full-tank mode was modeled in Ref. 4 by an annular tank with an assumed diameter ratio ( $k = \text{inside diameter/outside diameter}$ ) of 0.8. With this ratio, the  $\lambda$  for the 1<sup>st</sup> and 2<sup>nd</sup> mode of the full-tank slosh frequencies are predicted to be 1.1 and 15.8, respectively (see Table 1 of Ref. 20). For  $k = 0.5$ , the  $\lambda$  for the 1<sup>st</sup> and 2<sup>nd</sup> mode of the full-tank slosh frequencies are 1.35 and 6.6, respectively. As such, we have:

$$\omega_1^{\text{full-tank, } k=0.8} = 0.175 \sqrt{\frac{a}{R}} \text{ Hz}, \quad \omega_2^{\text{full-tank, } k=0.8} = 2.515 \sqrt{\frac{a}{R}} \text{ Hz} \quad (\text{A4})$$

$$\omega_1^{\text{full-tank, } k=0.5} = 0.215 \sqrt{\frac{a}{R}} \text{ Hz}, \quad \omega_2^{\text{full-tank, } k=0.5} = 1.050 \sqrt{\frac{a}{R}} \text{ Hz}$$

At the start of the PRM burn, the fill fractions of the tanks are 35%. The corresponding liquid depth is 0.608 m ( $h/R = 0.9806$ ). Again, the  $\lambda$  for the 1<sup>st</sup> and 2<sup>nd</sup> mode of the sector slosh frequencies are 3.84 and 5.29, respectively. Since  $\tanh(3.84 \times 0.9806) \approx \tanh(3.766) \approx 0.99893$ , and  $\tanh(5.29 \times 0.9806) \approx \tanh(5.187) \approx 0.99994$ , the resultant propellant slosh frequency expressions are identical to those given in Eq. (A3) (but with a different axial acceleration “a” at the time of the PRM burn). The 1<sup>st</sup> and 2<sup>nd</sup> full-tank modes for two different values of diameter ratio ( $k$ ) are also given by Eq. (A4).

## Appendix B

### An Oscillatory Spacecraft Z-axis Attitude Control Error Observed During RPWS Whistler Observations

During the Tour phase of the Cassini mission, RCS thrusters are sometimes used to control the S/C’s attitude. For example, to allow the RPWS to perform a “Saturn lightning whistler” observation, the reaction wheels must be turned off to eliminate any electro-magnetic interference caused by the RWA motors. The spacecraft was in a quiescent state as it pointed at the Earth. During all RPWS whistler observations, there wasn’t any torque imparted on the spacecraft due to articulation motions of the science instruments CDA and CAPS (Cosmic Dust Analyzer and Cassini Plasma Spectrometer, respectively) because they were both powered off. RPWS then ramped up their data-sampling rate and began “listening” for possible lightning storms on Saturn. In the year 2007–2008, a series of fifteen “RPWS Whistler” science observations were conducted. Time histories of the S/C’s per-axis attitude control errors of the RPWS whistler event conducted on 2008-DOY-004 are depicted in Fig. B1. A zoomed-in of the Z-axis attitude control error is also given in that figure. One can see clearly from these figures that superimposed on the low frequency “ping-ponging” motions of the attitude control errors about all axes are oscillatory attitude errors at a higher frequency, due to an unknown source(s). The oscillatory motion is most pronounced in the telemetry of the Z-axis attitude control error. The approximate frequency of the un-damped oscillatory motion was 2.5 mHz.

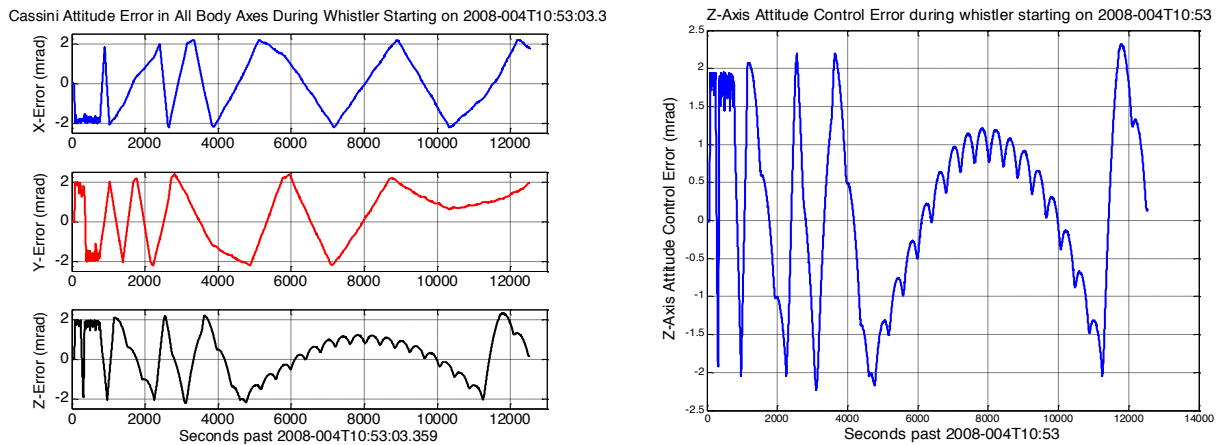


**Figure B1. Per-axis attitude control errors of the spacecraft on 2008-DOY-004**